Journal of Inflammation Research

Dovepress
open access to scientific and medical research

Open Access Full Text Article

ORIGINAL RESEARCH

RETRACTED ARTICLE: Ginsenoside Rg1 Inhibits Microglia Pyroptosis Induced by Lipopolysaccharide Through Regulating STAT3 Signaling

Yueyi Yao[1]
Changyan Li[1]
Fusheng Qian[1]
Yu Zhao[1]
Xiaoyi Shi[1]
Dan Hong[1]
Qinglong Ai[2]
Lianmei Zhong[2]

[1]Science and Technology Achievement Incubation Center, Kunming Medical University, Kunming, 650500, People's Republic of China; [2]Department of Neurology, First Affiliated Hospital of Kunming Medical University, Kunming, 650032, People's Republic of China

Purpose: Neuroinflammation runs through the whole process of nervous system diseases and brain injury. Inflammasomes are thought to be especially relevant to immune homeostasis, and their dysregulation contributes to pyroptosis. The natural compound Ginsenoside Rg1 has been shown to possess anti-inflammatory effects; however, its underlying mechanisms are not entirely clear. Therefore, this study was undertaken to investigate the role and mechanisms of Rg1 in regulating the production of inflammasomes and pyroptosis of microglia in vivo and in vitro.

Methods: BV-2 microglial cells were pretreated with Rg1, stattic and interleukin-6 (IL-6), and then stimulated with lipopolysaccharide (LPS) (2μg/mL). Hoechst staining and Annexin V-FITC/PI assay were then carried out. The expression levels of cleaved-caspase-1, pro-caspase-1, interleukin-1β (IL-1β), mature-IL-1β, gasdermin D (GSDMD), activated NH(2)-terminal fragment of GSDMD (GSDMD-N), NOD-, LRR- and pyrin domain-containing 3 (NLRP3) inflammasome, apoptosis-associated speck-like protein containing a CARD (ASC), absent in melanoma 2 (AIM2), signal transducer and activator of transcription 3 (STAT3) and phosphorylated STAT3 in BV-2 were detected by Western blotting. Additionally, immunofluorescence staining was used to determine the expression of NLRP3 and p-STAT3 in postnatal rat brain and BV-2 microglia subjected to LPS stimulation and Rg1 pretreatment. The targets of transcription factor STAT3 were predicted by hTFtarget and chromatin immunoprecipitation (ChIP) was used to confirm the interaction between STAT3 and AIM2.

Results: We showed here that Rg1 effectively inhibited the expression of inflammasomes and microglia pyroptosis induced by LPS. The targets predicted data of Rg1 from Swiss target prediction database showed STAT3 had the highest thresholds of probability score. Rg1 can regulate the phosphorylation of STAT3, which binds to the promoter region of inflammasome AIM2.

Conclusion: It is suggested that STAT3 signaling can initiate the transcription activity of AIM2. Rg1 regulates microglia pyroptosis in neuroinflammation induced by LPS through targeting STAT3 signaling.

Keywords: neuroinflammation, AIM2, microglia, pyroptosis, Rg1

Correspondence: Lianmei Zhong; Qinglong Ai
Department of Neurology, First Affiliated Hospital of Kunming Medical University, 295 Xichang Road, Kunming, 650032, Yunnan Province, People's Republic of China
Tel/Fax +86-0871-65336015
Email 13888967787@163.com; aiqinglong63@163.com

Introduction

Neuroinflammation is a complex innate immune response to various harmful stimuli viz., pathogens, damaged cells and irritants in the central nervous system (CNS). It is featured prominently in the pathogenesis process of different neurodegenerative diseases such as Multiple Sclerosis (MS), Parkinson's disease (PD) and Alzheimer's disease (AD).[1] There is strong evidence indicating that neuroinflammation is involved

Received: 8 July 2021
Accepted: 2 November 2021
Published: 7 December 2021

in the biochemical process when the brain is challenged by infection, traumatic, ischemic, reperfusion injuries and strokes.[2]

Microglia represent the major immunologically active glial cell type in the brain. They are widely distributed in the brain and are swiftly activated through innate immune receptors upon the introduction of various stimuli. It is well documented that activated microglia released a wide array of neurotoxic factors, such as IL-1β and interleukin-18 (IL-18).[3–5] The secretion of IL-1β in microglia is accompanied by the activation of inflammasome and pyroptosis, a process of inflammatory cell death.[6]

Inflammasome is a multiprotein complex composed of (1) a pattern recognition receptor (PRR) as the sensor molecule, (2) an adaptor protein ASC, and (3) a pro-caspase-1 as the effector molecule.[7] NLR is one of the PRRs.[8,9] Till date, at least five NLRs (NLRP1, NLRP3, NLRP6, NLRP7, and NLRC4) have been reported to participate in forming inflammasomes.[10,11] NLRP3, the most widely studied inflammasome, appears to be primarily expressed in microglia and is probably responsible for microglia activation.[12,13] NLRP3 inflammasome mediates stimuli triggering PRR protein oligomerization and recruits pro-caspase-1 into the complex, resulting in the activation of neighbor caspase-1. However, AIM2 is also a part of inflammasome which owns a HIN200 domain and a pyrin domain, but it does not belong to the NLRs. AIM2 recruits ASC through pyrin domain which binds to caspase-1 via CARD–CARD interaction.[14] Consequently, caspase-1 cleaves the biologically inactive pro-IL-1β and pro-IL-18 into mature cytokines that are then secreted by the cells.[15,16]

Apart from their role playing in the maturation of IL-1β, IL-18 and caspase-1, they can also induce a pro-inflammatory form of cell death, namely, pyroptosis, whose characteristic features include early plasma membrane rupture and releasing of soluble intracellular fraction and fueling the inflammatory response.[8] GSDMD is the executioner protein which perforates the plasma membrane resulting in cell swelling, membrane rupture and releasing pro-inflammatory cytokines.[17] The process of pyroptosis is accompanied by the further release of IL-1β, which exacerbates the inflammatory response.[18,19]

The effects of the released proinflammatory cytokines will be propagated and amplified by the signal transducer and activator of transcription (STAT) signaling pathways.[20] Phosphorylated STATs dimerize and translocate into the nucleus, where binding to conserved genomic regulatory sequences and controlling the expression of a multitude of genes.[21] STAT comprises seven isoforms (STAT1, STAT2, STAT3, STAT4, STAT5A, STAT5B and STAT6), and of which, STAT3 is considered the most-ancient and most-conserved isoform. Previous studies have reported that STAT3 phosphorylation is up-regulated in activated microglia and which might be linked to the major functions of activated microglia such as release of chemokines and cytokines following focal cerebral ischemia in rodents[22–24]; however, the functional significance of STAT3 activation in neuroinflammation and immune cell pyroptosis have remained obscure. It is therefore desirable to further investigate and ascertain whether neuroinflammation might be inhibited by regulating STAT3 signaling.

Ginsenoside Rg1 (Rg1) is one of the essential components of ginsen, and its neuroprotective effect has been widely reported. The neuroprotective effect of Rg1 may be related to its anti-inflammatory and anti-oxidation properties.[25] Our previous studies have demonstrated that Rg1 can protect against LPS-induced inflammation in murine BV2 microglial cells via the phospholipase C-γ1 signaling pathway.[26] Gao et al reported that Rg1 exerts anti-inflammatory effects via G-protein-coupled estrogen receptor in LPS-induced microglia activation.[27] Thus far, most studies on Rg1 have focused on its regulation of microglia activation; yet, surprisingly, the underlying mechanism that governs Rg1 anti-inflammatory effect has remained elusive. Therefore, this study was undertaken to unravel the underlying mechanism of Rg1 in microglia inflammatory death form-pyroptosis in microglia-mediated neuroinflammation. We show here that Rg1 endowed with its anti-inflammatory property can regulate microglia pyroptosis. Thus, the results have provided a further scientific basis for our better understanding and continuing investigation of Rg1 as a therapeutic agent for neurological diseases in which microglia-mediated neuroinflammation is implicated.

Materials and Methods

BV-2 Cells Culture and Treatment

The microglial cell line BV-2 cells was purchased from BeNa Culture Collection (Beijing, China, Resource ID: BNCC337749) and maintained at 37°C in a humidified incubator with 5% CO_2. The components of the culture medium contained Dulbecco's Modified Eagle medium (DMEM) (10013057, Corning, USA), 10% fetal bovine serum (FBS) (Cat. No. 04-001-1ACS, Biological

Industries, BI, USA) and antibiotics (100IU/mL penicillin and 100mg/mL streptomycin), (Invitrogen, Carlsbad, CA, United States). Rg1 was purchased from Kunming Pharmaceutical Corporation (Kunming, China) and its purity was more than 99%. Rg1 at the concentration of 20μM and 60μM was added 1h before LPS (2μg/mL) (Cat. No. L4391, Sigma-Aldrich, MO, USA) stimulation. The specific STAT3 inhibitor, stattic (10μM) (Cat. No. S7024, Selleck Chem, China), was used to determine if STAT3 signaling might be involved in the process of microglia pyroptosis. IL-6 (Cat. No. 216-16, PeproTech, China) was used to increase STAT3 signaling to determine the role of Rg1 in regulating microglia pyroptosis through STAT3 signaling.

Hoechst Staining

Hoechst nuclear staining was performed as described earlier[28] and modified slightly. Briefly, BV-2 microglia (10^6 cells/mL) were incubated for 10 min at 4°C with Hoechst 33342 dye (5μL) and PI (5μL) (CA1120, solarbio, Beijing, China) in dark. The morphology of the stained BV-2 microglia was visualized using a photomicroscope (Olympus) equipped with a fluorescent light source and a UV-2A filter cube. The experiments were repeated at least three times, and the percentage of PI-positive cells was calculated.

Construction of an Rg1 Target Network

We predicted the targets of Rg1 using the Swiss target prediction database (http://www.swisstargetprediction.ch/), and selected the crucial targets of Rg1 according to the screening threshold of probability score ≥0.02. Then we acquired the protein-protein interaction (PPI) network of the crucial targets from the String database (https://string-db.org/). Finally, resultant data were introduced into Cytoscape (v3.7.1) to construct the target-PPI network of Rg1's crucial targets.

Flow Cytometry

Annexin V-FITC/PI detection kit (A211-01, Vazyme, Nanjing, China) was performed according to the manufacturer's protocol. Both the supernatant and adherent were collected and centrifuged. Then, the cell pellets were resuspended in 100μL 1×binding buffer containing 5μL Annexin V-FITC and 5μL PI and incubated for 15min. Cells were examined by flow cytometry (BD C6).

Immunoblotting

For immunoblotting analysis, each group of BV-2 cells was dissolved in RIPA lysis buffer. The protein level was quantified using a BCA protein assay Kit (Cat. No. PC0020, Solarbio). Forty microgram protein extract was subjected to SDS-polyacrylamide gel electrophoresis (SDS-PAGE) and transferred onto immunoblot polyvinylidene difluoride membranes (PVDF membranes). The membranes were incubated with 5% non-fat milk for 2h. The membranes were then incubated with antibodies against cleaved-caspase-1, GSDMD, GSDMD-N, caspase-1, mature-IL-1β, NLRP3, ASC, IL-1β, STAT3, p-STAT3, AIM2 and β-actin antibodies at 4°C overnight, respectively. Catalogue numbers of antibodies used are given in Table 1. Then, the membranes were washed with TBST and incubated with secondary antibody for 2h at room temperature. Immunoblotting was performed using an enhanced chemiluminescence light-detecting kit (Millipore, Rockford, IL, USA) and the signals were captured using AI600 from GE Healthcare (Buckinghamshire, UK) and the optical density of each protein band was quantified by ImageJ software. The relative density of the protein bands was normalized with corresponding β-actin density.

Bioinformatics Analysis

As STAT3 is a transcription factor that can modulate the expression of target genes by binding to specific DNA sequences of their promoter(s) or enhancer(s). The specific DNA sequences of promoter(s) or enhancer(s) that STAT3 binding was predicted by hTFtarget database (http://bioinfo.life.hust.edu.cn/hTFtarget). JASPAR website (http://jaspar.genereg.net/sites/MA0093.2/) was searched to identify STAT3 binding sites in AIM2. As previously reported, the species was selected, and the relative profile score threshold was set to 80% to scan the target DNA sequence.[29]

Chromatin Immunoprecipitation (ChIP)

ChIP was performed using Chromatin Immunoprecipitation Kit (Cat No. P2078, Beyotime, China). As described previously,[30] cells were cross-linked by formaldehyde at 37°C. Glycine was added to stop cross-linking for 5 min at room temperature. The cells were washed and collected with cold PBS with PMSF. After centrifugation at 1000g for 5 min at 4°C, pellets were dissolved by SDS lysis buffer with 1mM PMSF.

Table 1 Antibodies Used for Immunofluorescence and Western Blotting

Antibody	Host	Source	Catalog Number	Dilution for Staining	Dilution for Western Blot
NLRP3	Rabbit polyclonal	Abclonal, China	WH110563	1/200	1/1000
Cleaved-caspase-1	Rabbit polyclonal	Cell Signaling Technology	4199s		1/1000
ASC	Rabbit polyclonal	Cell Signaling Technology	67824s		1/1000
β-Actin	Mouse monoclonal	Proteintech	66009-1-Ig		1/4000
STAT3	Mouse monoclonal	Cell Signaling Technology	9139s		1/1000
p-STAT3	Rabbit polyclonal	Cell Signaling Technology	9145s	1/100	1/1000
GSDMD	Rabbit polyclonal	Proteintech	20770-1-AP		/2000
IL-1β	Rabbit polyclonal	Cell Signaling Technology	31202		000
AIM	Rabbit polyclonal	Affinity	DF3514		1/1000
Lectin	Lycopersicon esculentum	Sigma-Aldrich, USA	L0401	1/200	
DAPI		Sigma-Aldrich, USA	057		
Mature-IL-1β	Rabbit polyclonal	Cell Signaling Tech	8318		1/1000
Pro-caspase-1	Rabbit polyclonal	Cell Signaling chnology	24232		1/1000
GSDMD-N	Rabbit polyclonal	Cell Signaling chnology	36425		1/1000
Goat anti-rabbit IgG H&L (Alexa Fluor® 647) preadsorbed	Goat anti-rabbit	Abcam	Ab150083	1/500	
Horseradish peroxidase conjugated secondary antibody	Goat anti-rabbi	inity	s0001		1/2000
Horseradish peroxidase conjugated secondary antibody	Goat -mouse	ffinity	s0002		1/2000

Sonicated was used for DNA fragmenta n. Then, 200μL cell lysate from each gro was diluted to 2 L with ChIP dilution buffer and 20 was t en as input samples. The rest of the liquid was in ted sepa ely with antibody against STAT3 nd I G cont l an body overnight at 4°C. The next d protei A+G Aga ose/Salmon Sperm DNA was added to re pitate the antibody-protein-DNA complexes for 1h at °C. Subsequently, the complexes were washed with corresp nding solutions. After all the above washing steps, the precipitate was eluted by the elution buffer composed of 1% SDS and 0.1M $NaHCO_3$. Eluate (500μL) and input were supplemented with NaCl, mixed and heated at 65°C for 4h to remove the cross-linking between the protein and genomic DNA. Afterwards, proteins were digested with proteinase K (20μg/μL, BioFroxx, Germany) and DNA was isolated and purified by DNA purification kit according to the instruction. The purified DNA was dissolved in 50μL H_2O. Promoter-specific primers used were mouse AIM2-1: 5′-GGAAATACACCC TGCTTGA-3′ (Forward), 5′-ACTCCAGTTGGGAAACC AC-3′ (Reverse); AIM2-2: 5′-TGCCTTTCCAGGACCT CTT-3′(Forward), 5′-ACCAACTCTCTCCCTCACTCTG -3′(Reverse); AIM2-3: 5′-GCCTTTCCAGGACCTCTTT -3′(Forward), 5′-AACTCTCTCCCTCACTCTGCTA-3′ (Reverse). AIM2-4: 5′-TGGTTTCTCACCTTGACT GG-3′ (Forward), 5′-TACTGGCAGGAGCAGGATT-3′ (Reverse). The DNA level of AIM2 was measured by RT-PCR.

Animal Experiment

Sprague Dawley rats aged 3 days were used for animal experiment. The healthy animals were randomly divided into control group, LPS treatment group and Rg1 intervention group (n = 3, at each group). The rats in Rg1

treatment group were given Rg1 100mg/kg treatment 1h before LPS (1mg/kg) injection administrated intraperitoneally. In the LPS group, the rats were performed intraperitoneal injection with LPS (1mg/kg). The rats were sacrificed at 6h after LPS injection.

The rats were anesthetized with sodium pentobarbital and perfused transcardially with PBS followed by 4% paraformaldehyde in 0.1M phosphate buffer, pH 7.4. Following perfusion, the brains were removed and further fixed in paraformaldehyde at 4°C overnight. After that, the tissue samples were dehydrated with 30% sucrose at 4°C overnight. For immunostaining, the brains were rapidly frozen and sectioned coronally at 13μm thickness through the forebrain with a cryostat (Model CM 3050; Leica Instruments GmbH, NUBLOCH, Germany). Brain sections were mounted onto slides and stored at −20°C until use.

All experiments were carried out in accordance with the National Institute of Health Guide for the Care and Use of Laboratory Animals (NIH Publications number 80-23). The project was approved by the Department of Science and Technology, Yunnan Province, China.

Double Immunofluorescence Labeling

BV-2 microglia in each treatment group were fixed with 4% paraformaldehyde in 0.1M PBS for 20min. After washing with PBS, the cells were sealed with 5% goat serum for 2h. Following this, the cells were incubated in antibodies against NLRP3 and p-STAT3 overnight. Subsequently, for BV-2 cells, cells were incubated with goat anti-rabbit IgG H&L (Alexa Fluor® 647) and lectin (dilution 1:200) cocktail for 2h at 37°C. Catalogue numbers of antibodies used are given in Table 1. All images were captured with a fluorescence microscope (Olympus, BX53).

For the rat brain double immunofluorescence staining, coronal brain sections at 13μm thickness were rinsed in PBS and then incubated with 5% goat serum for 2h. After serum blocking, tissue sections were incubated with primary antibodies against NLRP3 and p-STAT3 at 4°C, respectively. The unbound antibody was washed with PBST. After that, sections were incubated with a mixture of secondary antibodies: FITC-conjugated lectin and goat anti-rabbit IgG H&L (Alexa Fluor® 647) for 2h. Finally, brain sections were stained with DAPI. Images were acquisitied by confocal microscope (Zeiss, LSM880).

Lectin-positive microglia in the corpus callosum of different groups were counted at ×200 magnification. The expression of the target protein is expressed as positive cell count per unit area (expressed in terms of percentage). In BV-2 microglia, quantification of cellular immunofluorescence intensity in the fluorescence images was expressed as optical density, which was quantified using ImageJ software; changes in intensity were then plotted.

Statistical Analysis

Data were shown as the mean ± SD. They were obtained from three independent experiments and evaluated with Graph Pad Prism Version 6.0 software (San Diego, CA, USA). The significance of difference between groups was determined by Student's independent samples *t*-test or one-way analysis of variance (ANOVA) followed by Tukey's post hoc test. $p < 0.05$ was considered statistically significant.

Results

Ginsenoside Rg1 Inhibited Microglia Pyroptosis Induced by LPS

Rg1 exerts diverse cell bioactivities, including regulating proliferation, apoptosis and migration.[31,32] To investigate whether Rg1 is involved in the regulation of microglia pyroptosis and its potential mechanism. BV-2 cells were stimulated with LPS. Rg1 was administered prior to LPS stimulation. Hoechst 33342/PI staining analysis indicated that the percentage of PI-positive cells of LPS-induced BV-2 cells was higher than that in the control group, and which was attenuated by Rg1 treatment (Figure 1A and B).

Pyroptosis is characterized by the rapid loss of the plasma membrane integrity; hence, membrane-impermeable dyes like PI will stain the pyroptic cell. On the other hand, Annexin V binds to phosphatidyl, which is localized to the inner leaflet of the cell membrane. Annexin V-FITC/PI double-staining showed that LPS treatment resulted in a significant increase in the percentage of early apoptotic and necrotic or late apoptotic cells (about 5.8%) compared to the control group (Figure 1C and D); however, pretreatment with Rg1 at the concentration of 20μM and 60μM significantly reduced the percentage of early apoptotic and necrotic or late apoptotic cells.

The above results, however, could not fully determine the occurrence of pyroptosis. Therefore, expression of pro-caspase-1, cleaved-caspase-1, GSDMD, GSDMD-N, IL-1β and mature IL-1β was further detected. As shown in Figure 1E–K, the levels of

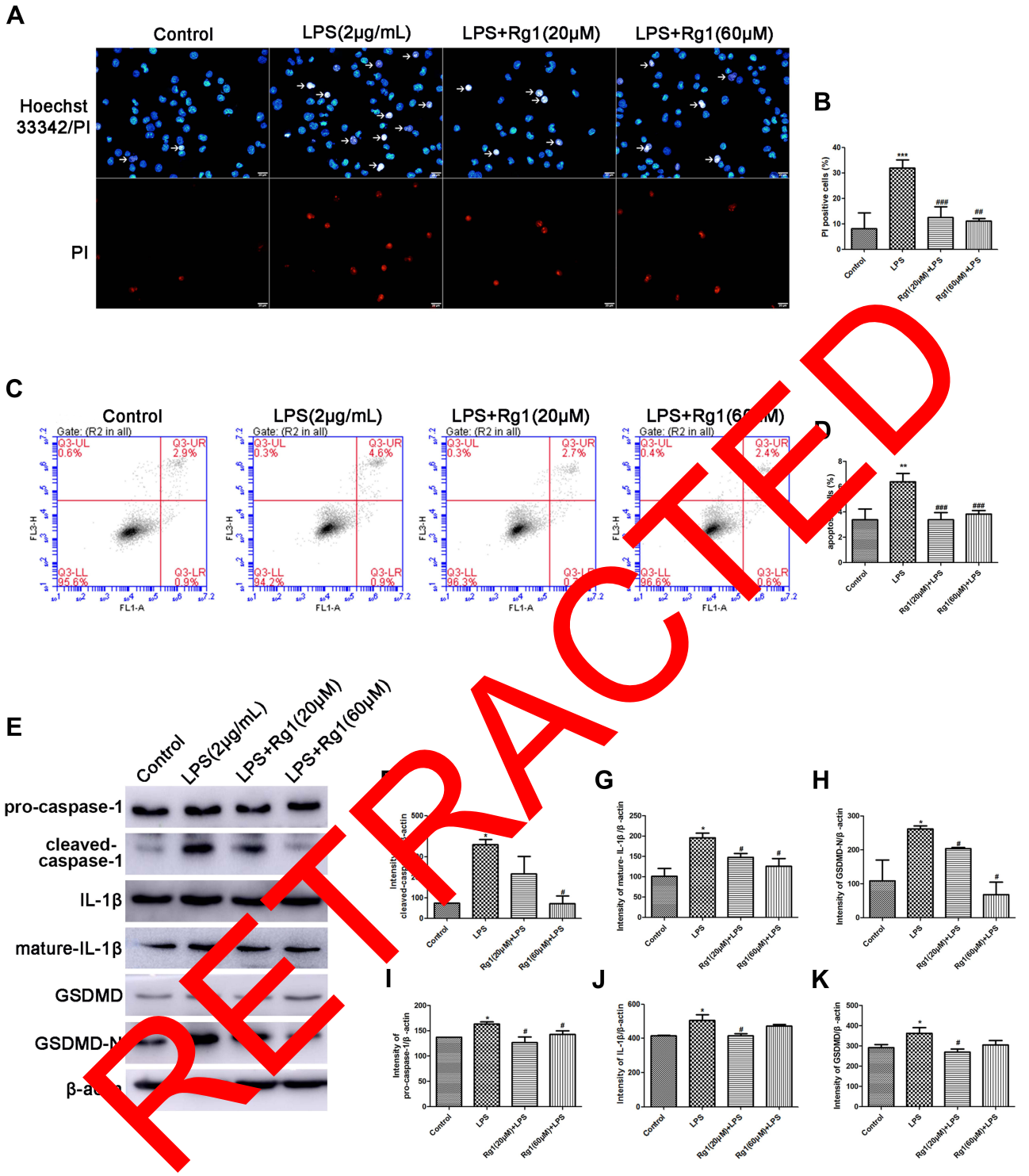

Figure 1 Rg1 inhibits pyroptosis induced by LPS in BV-2 microglia. (**A**) BV-2 microglia pyroptosis was observed via Hoechst 33342/PI double staining (magnification, x200), dead nuclei were stained pink or bright red. Arrows indicate PI-positive cells. Scale bar= 20μm. (**B**) The calculated percentage of PI-positive cells. All values are expressed as mean ± SD (n = 3 per group). $^{***}p < 0.001$ compared with the control group, $^{\#\#}p < 0.01$ and $^{\#\#\#}p < 0.001$ compared with the LPS group. (**C**) The incidence of apoptosis cells was examined by flow cytometry. Rg1 (20 and 60μM) down-regulated the rate of apoptosis induced by LPS. Compared with the cells pretreated with Rg1 (20 and 60μM), the rate of apoptosis was markedly increased with LPS treatment for 24h. (**D**) Bar graph shows the total rate of apoptosis in each group. $^{**}p < 0.01$ compared with the control group, $^{\#\#\#}p < 0.001$ compared with the LPS group. (**E**) BV-2 microglia were pretreated with or without Rg1 (20 and 60μM) for 1h and co-cultured with LPS at 2μg/mL for 12h. Western blot analysis shows protein expression levels of cleaved-caspase-1, pro-caspase-1, IL-1β, mature-IL-1β, GSDMD and GSDMD-N. (**F**–**K**) Bar graph shows gray value analysis based on immunoblot images. $^{*}p < 0.05$ compared with the control group, $^{\#}p < 0.05$ compared with the LPS group.

cleaved-caspase-1, GSDMD-N and mature IL-1β were markedly increased in LPS-induced BV-2 microglia compared with control. Remarkably, the expression levels of the biomarkers mentioned above were inhibited by Rg1 treatment. Of note, the concentration of Rg1 at 60μM exerted a more stable or consistent effect. It has been reported that mature-IL-1β and cleaved-caspase-1 can induce pyroptosis, while, GSDMD is the executioner protein that ruptures membrane and results in pro-inflammatory cytokines releasing.[17]

Ginsenoside Rg1 Inhibited the Production of Inflammasome Induced by LPS in Microglia

It is well documented that the production of intracellular inflammasomes is closely related to pyroptosis. In this connection, NLRP3 acts as an inflammatory body to mediate pyroptosis.[33,34] ASC as a linker protein that connects intracellular receptors and caspase-1 in inflammatory bodies; pyroptosis is triggered after its activation by various inflammasomes.[35] Thus, to explore the expression of inflammasomes, Western blot was performed to measure the protein expression levels of NLRP3 and ASC in BV-2 microglia. The results showed that the protein expression levels of NLRP3 and ASC were up-regulated in LPS-induced BV-2 cells compared with control, and these were inhibited by Rg1 (Figure 2A–C). Furthermore, the expression of NLRP3 was detected by immunofluorescence staining, which is the most widely studied inflammasome expressed in activated microglia.[12,13] As shown in Figure 2D, the lectin-labeled BV-2 microglia exhibited co-expression of NLRP3 in their cytoplasm in LPS treatment group. On the other hand, increased expression of NLRP3 induced by LPS was obviously attenuated by Rg1 at the concentration of 20μM and 60μM being more drastic in the latter (Figure 2D and E).

By immunofluorescence staining, NLRP3 expression was hardly detected in lectin-labeled microglia in the corpus callosum of control postnatal rats. However, in LPS-injected group, the number of lectin-labeled microglia with enhanced NLRP3 expression was significantly increased. Conversely, in LPS-injected group given Rg1 pretreatment, NLRP3 expression in lectin-labeled microglia was significantly decreased (Figure 2F and G).

Ginsenoside Rg1 Inhibited the Phosphorylation of STAT3 Induced by LPS in Activated Microglia

The targets of Rg1 were predicted by Swiss target prediction database (http://www.swisstargetprediction.ch/). According to the screening thresholds of probability score (≥0.02), 17 hub-targets (STAT3, IL-2, PTAFR, VEGFA, FGF1, FGF2, HPSE, ATP1A1, TYMS, PSEN2, TACR2, HSP90AA1, IGF1R, LGALS4, LGALS3, LGALS8, OPRD1) were selected. The protein–protein interaction (PPI) network of the 17 targets was acquired from the String database (https://string-db.org/). Resultant data were introduced into Cytoscape (v3.2.1) to construct the target-PPI network of Rg1's 17 targets (Figure 3A). Among them, STAT3 obtained the highest probability score, 0.08.

According to the predicted results, the role of Rg1 in regulating the STAT3 needs to be further confirmed. Western blotting results showed that Rg1 inhibited the phosphorylation at tryptophan 705 (Tyr705) of STAT3 significantly in activated BV-2 microglia induced by LPS (Figure 3B).

By immunofluorescence labeling, the expression of STAT3 was initially detected in the cytoplasm in the absence of stimuli. As shown in Figure 3C, STAT3 was phosphorylated and translocated into the nucleus in activated BV-2 microglia induced by LPS. Of note, Rg1 significantly inhibited the phosphorylation of STAT3 and its nuclear translocation (Figure 3C and D). Consistent with the results in vitro, immunoexpression changes in p-STAT3 were also observed in activated microglia in the corpus callosum of 3-day-old postnatal rats challenged with LPS. p-STAT3 immunofluorescence intensity in lectin-labeled microglia was decreased by Rg1 treatment at the dose of 100mg/kg (Figure 3E and F).

Ginsenoside Rg1 Inhibited Microglia Pyroptosis Though STAT3 Signaling

As a transcription regulator, STAT3 might act a novel regulator of inflammasome production. First, the genes binding by STAT3 were predicted through the hTFtarget database and AIM2 was selected as the object. Next, the JASPAR bioinformatics prediction website was used to analyze the binding relationship between STAT3 and AIM2 promoter and four possible binding sites were found (Figure 4A and B). Finally, ChIP assay verified the interaction of STAT3 protein with AIM2 gene

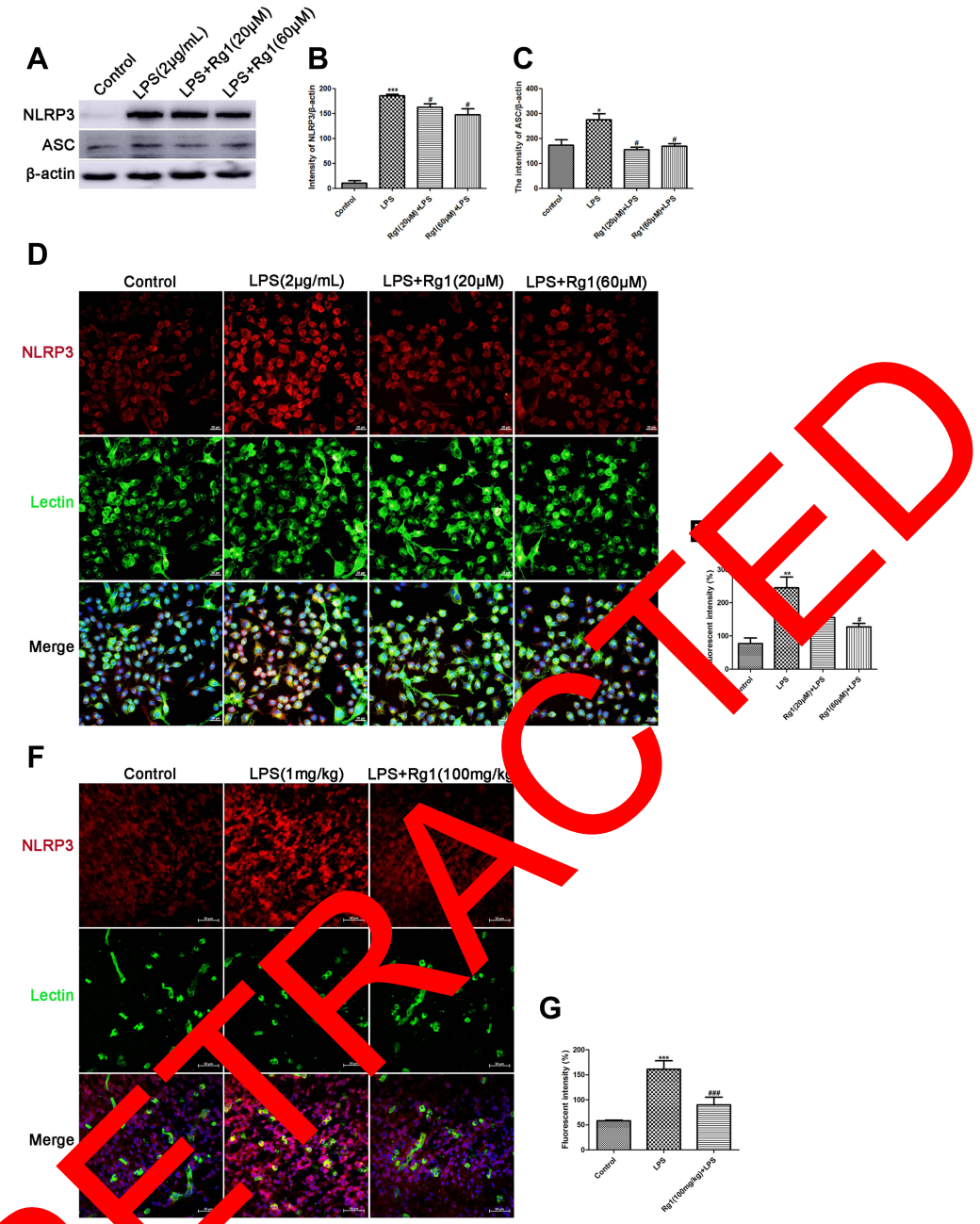

Figure 2 Rg1 inhibits the production of inflammasomes induced by LPS in BV-2 microglia. (**A**) Rg1 at 20 and 60μM was added to BV-2 cells before stimulation with LPS at 2μg/mL and incubated for 1 h. Western blot analysis shows the protein expression levels of ASC and NLRP3. (**B** and **C**) Bar graphs show gray value analysis based on immunoblot images. $^{*}p < 0.05$ and $^{***}p < 0.001$ compared with the control group, $^{\#}p < 0.05$ compared with the LPS group. (**D**) Immunofluorescence images showing NLRP3 expression (red) in lectin-positive microglia (green) in BV-2 microglia. DAPI-blue. Scale bars=20μm. (**E**) Bar graph shows fluorescent intensity analysis, $^{**}p < 0.01$ compared with the control group, $^{\#}p < 0.05$ compared with the LPS group. (**F**) Immunofluorescence images showing NLRP3 expression (red) in lectin-positive microglia (green, arrows) in the corpus callosum of postnatal brain. DAPI-blue. Scale bars=50μm. (**G**) Bar graph shows fluorescent intensity analysis, $^{***}p < 0.001$ compared with the control group, $^{\#\#\#}p < 0.001$ compared with the LPS group.

promoter using primers specific to AIM2 (Figure 4C). Site1, rather than site2, site3 or site4, was considered the binding site of STAT3 on the AIM2 promoter region. Compared to the control group, LPS increased the binding of endogenous STAT3 to the AIM2 promoter at site1 in BV-2 cells. Mouse IgG was used as the negative control to exclude nonspecific binding in all the experiments. Thus, it is suggested that STAT3 may regulate the inflammasome production by targeting the promoter of AIM2 and induce transcriptional activation of AIM2.

STAT3 phosphorylation at Tyr705 in the α-subunit is a key mechanism in mediation of STAT3 activation.[22] To

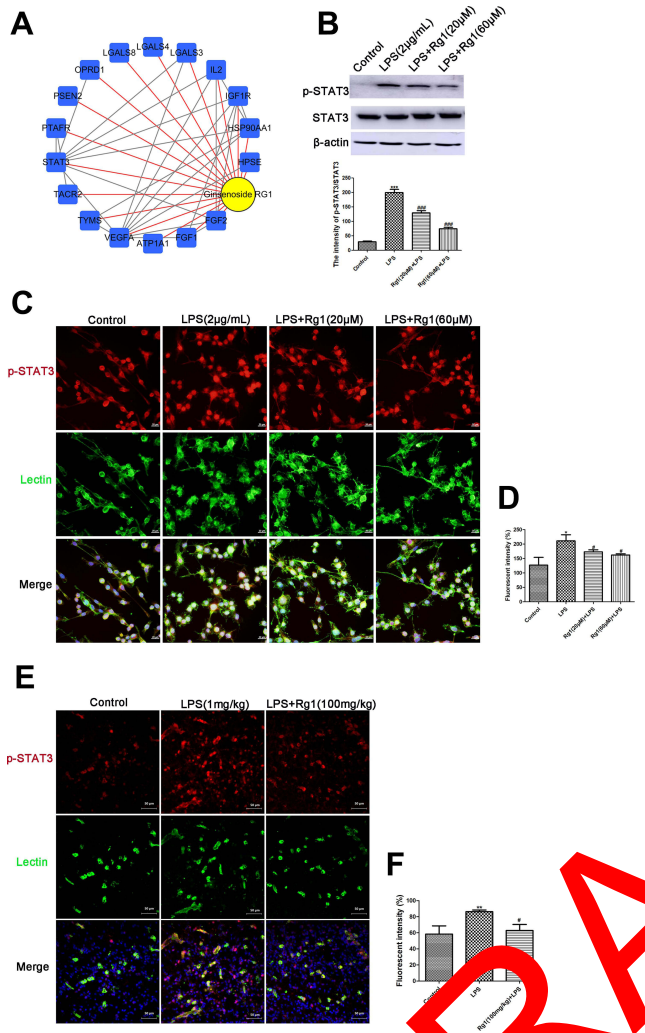

Figure 3 Rg1 inhibits the phosphorylation of STAT3 induced by LPS in BV-2 microglia. (**A**) The target-PPI network of Rg1. As depicted, 18 crucial targets of Rg1 were identified. They are represented by the blue rounded squares. In addition, the yellow ellipse represents Rg1. The red edge denotes the relationship between Rg1 and targets, while the the gray edge represents the PPI among Rg1's targets. The network contains 18 nodes that are interconnected and associated with 41 edges. (**B**) Western blotting results showing phosphorylation of STAT3 in LPS-activated BV-2 microglial cells with or without Rg1 (20 and 60μM) pretreatment. Bar graph shows the gray value analysis based on immunoblot images. ***$p < 0.001$ compared with the control group, ###$p < 0.001$ compared with the LPS group. (**C**) Immunofluorescence images showing STAT3 expression (red) in lectin-positive microglia (green, arrows) in BV-2 microglia. DAPI-blue. Scale bars=20μm. (**D**) Note the enhanced expression of NLRP3 in activated microglia, which is noticeably attenuated by Rg1 treatment. **$p < 0.05$ compared with the control group, #$p < 0.05$ compared with the LPS group. (**E**) Immunofluorescence images showing STAT3 expression (red) in lectin-positive microglia (green, arrows) in the corpus callosum of postnatal brain. DAPI-blue. Scale bars=50μm. (**F**) Note enhanced expression of NLRP3 in activated microglia, which is obviously attenuated by Rg1 treatment. **$p < 0.01$ compared with the control group, #$p < 0.05$ compared with the LPS group.

further explore the connection between STAT3 and pyroptosis in microglia, Western blot was performed and the results showed that the levels of NLRP3, AIM2, ASC, cleaved-caspase-1, pro-caspase-1, GSDMD, GSDMD-N, mature-IL-1β and IL-1β proteins in LPS-induced BV-2 cells were increased, which was inhibited by stattic which serves as STAT3 inhibitor (Figure 4D–M). Further, the ratio of early apoptotic and necrotic or late apoptotic cells in the LPS group was higher than that in the control group; stattic repressed this level (Figure 4N). This indicates that STAT3 is associated with microglia pyroptosis, and that Rg1 shared the same effect as stattic.

Along with the above, Western blot analysis also indicated that IL-6, the STAT3 agonist, neutralized the effect of Rg1 on down-regulating the protein expression of NLRP3, AIM2, ASC, cleaved-caspase-1, pro-caspase-1, GSDMD, GSDMD-N, mature-IL-1β and IL-1β (Figure 4D–M). Annexin V-FITC/PI double-staining results showed that the ratio of apoptotic cells in IL-6 +LPS+Rg1 group was higher than that in LPS+Rg1 group (Figure 4N and O). Thus, IL-6 abrogated the role of Rg1 in down-regulating pyroptosis induced by LPS in BV-2 microglia. The present results showed that STAT3 could interact with AIM2, and ginsenoside Rg1 inhibited microglia pyroptosis induced by LPS through regulating STAT3 signaling.

Discussion

Neuroinflammation is a complex innate immune response to various harmful stimuli such as pathogens, damaged cells and irritants in the central nervous system (CNS).[1] Among the various glial cell types, microglia have been well documented to play a pivotal role in the innate CNS immune response by facilitating neuroprotection and repair processes against invading pathogens.[36] Therefore, modulating microglia activation is deemed an important therapeutic strategy so that effective specific therapeutic drugs and strategies may be identified for mitigation of microglia-mediated neuroinflammation in different CNS diseases. In the present study, we have shown the occurrence of pyroptosis and expression of intracellular inflammasome in BV-2 microglia as well as in microglia in the corpus callosum in the postnatal rats subjected to LPS exposure unequivocally. A significant finding was that STAT3 signaling was activated in LPS-activated microglia; additionally, we have shown that microglia pyroptosis was decreased by inhibiting STAT3. More importantly, we have shown that Rg1 can regulate pyroptosis via STAT3 signaling (Figure 5). Arising from these, the role and underlying mechanisms of Rg1 in regulating microglia pyroptosis are now better clarified. This has provided the cellular and molecular bases for Rg1 for its potent

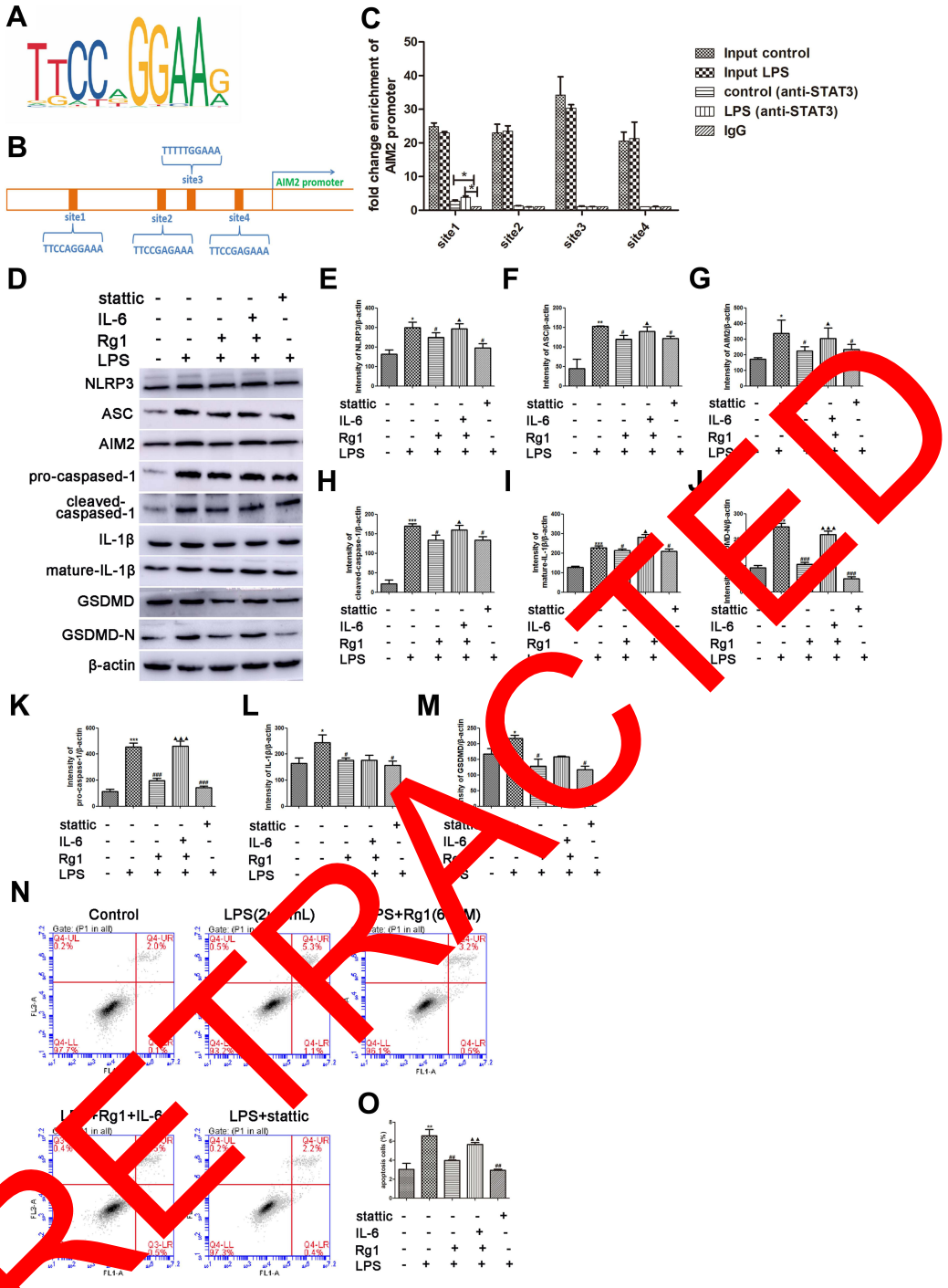

Figure 4 Rg1 inhibits pyroptosis through STAT3 signaling. (**A**) Conserved sequences at binding sites of STAT3. (**B**) STAT3 binding sites on AIM2 promoters predicted by JASPAR. (**C**) The binding relationship between STAT3 and AIM2 promoter verified by ChIP-qPCR experiment. *$p < 0.05$ compared with IgG negative control. (**D**) Western blotting analysis showing NLRP3, ASC, AIM2, cleaved-caspase-1, pro-caspase-1, IL-1β, mature-IL-1β, GSDMD and GSDMD-N protein expression in BV-2 cells with or without Rg1 pretreatment exposed to LPS or LPS with IL-6 stimulation, and with or without stattic treatment induced by LPS. (**E**–**M**) Bar graph shows gray value analysis based on immunoblot images. *$p < 0.05$, **$p < 0.01$, ***$p < 0.001$ compared with control, $^{\#}p < 0.05$ and $^{\#\#\#}p < 0.001$ compared with LPS treatment group, $^{\Delta}p < 0.05$ and $^{\Delta\Delta\Delta}p < 0.001$ compared with LPS+Rg1 treatment group. (**N**) Flow cytometry shows the percentage of dead cells over total cells in each stage. The effect of Rg1 (60μM) in down-regulating the rate of apoptotic cells induced by LPS was abrogated by IL-6. Compared with LPS (2μg/mL) treatment group, the rate of apoptotic cells was markedly decreased in stattic and LPS co-incubated group. (**O**) Bar graph shows the statistical results of the rate of dead cells in each group. **$p < 0.01$ compared with control, $^{\#\#}p < 0.01$ compared with LPS treatment group, $^{\Delta\Delta}p < 0.01$ compared with LPS+Rg1 treatment group.

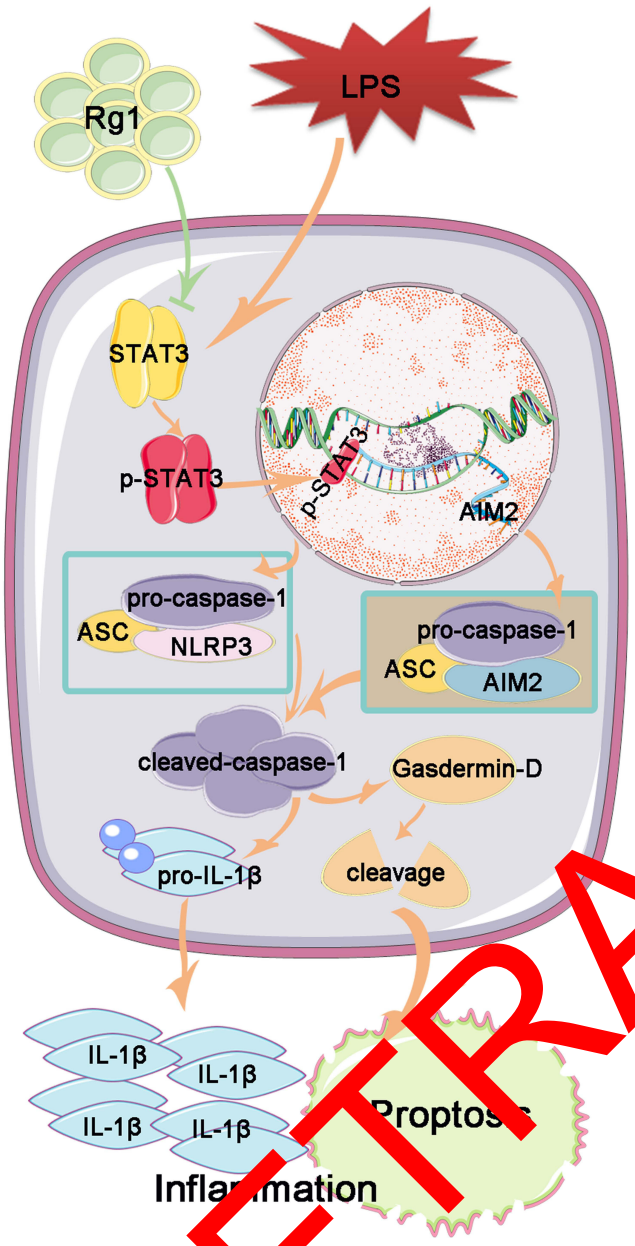

Figure 5 A schematic diagram depicting the proposed signaling mechanism via which Rg1 can exert its neuroprotection effect on lipopolysaccharide (LPS)-induced microglia pyroptosis. Following LPS stimulation, phosphorylated STAT3 (Tyr705) translocates into the nucleus and binds to the promoters of related genes such as AIM2 inflammasome. AIM2 transcription is initiated and forms inflammasome complexes with ASC and pro-caspase-1. Activated caspase-1 mediates the maturation of IL-1β, and the cleaved N-terminal of GSDMD triggers pyroptosis. However, phosphorylation of STAT3 enhanced the expression of NLRP3. NLRP3, ASC and pro-caspase-1 are assembled into inflammasome complexes and mediate microglia pyroptosis. Rg1 disrupts the pathway and protects against LPS-induced microglia pyroptosis and inflammatory response through inhibition of STAT3 signaling.

therapeutic treatment of microglia-mediated neuroinflammatory disease.

STATs are involved in different cellular activities including the activation and inflammation response of microglia induced by LPS.[37] Studies have shown that in the process of neuronal development, neuroprotection and nervous system inflammation, STAT3 is activated in different brain cells such as neurons, astrocytes and microglia, etc.[38] It is relevant to note that STAT3 is activated in microglia with LPS stimulation in the present results. In view of this, it was suggested that STAT3 might be linked to the fate of activated microglia such as inflammation-mediated cell death-pyroptosis, but the specific functional role of the transcription factor in microglia remains uncertain. The results of bioinformatics analysis showed that the activation of STAT3 could be regulated by Rg1 (Figure 3A and B). Furthermore, Western blot analysis confirmed that Rg1 at 20μM and 60μM effectively inhibited the phosphorylation of STAT3 at Tyr705 induced by LPS. Here, we extended the study and demonstrated additional roles of microglial STAT3, such as its ability to mediate the production of inflammasome and the pyroptosis of microglia, and the relationship between the neuroprotective effect of Rg1 and its regulation of STAT3.

During neuroinflammation, activated microglia lead to clearance of debris or invading pathogens, and release of neurotrophic factors that regulate the microenvironment.[39,40] Subsequently, the proinflammatory cytokine IL-1β, which was a crucial contributor to the brain injury, was facilitated and released through a caspase-1 dependent form of cell death-pyroptosis.[41] Pyroptosis is an inflammatory form of cell death. GSDMD is a well-known substrate for all inflammatory caspases and is cleaved by caspase-1 forming GSDMD-N. The GSDMD-N oligomerized in the plasma membrane and resulted in cell swelling and osmotic lysis.[19,42] Additionally, He et al demonstrated that cells lacking GSDMD could not undergo pyroptotic cell death or secrete the processed IL-1β.[43] We showed here that LPS increased the expression of GSDMD-N, cleaved-caspase-1 and IL-1β. Based on this premise, we adopted stattic to inhibit the activation of STAT3 signaling to further elucidate its role in the process of microglia pyroptosis. Remarkably, inhibition of STAT3 decreased the expression of GSDMD-N, cleaved-caspase-1 and IL-1β despite the stimulation of LPS, suggesting that STAT3 may have a regulatory effect on microglial pyroptosis.

The present results have shown that Rg1 shared the same inhibitory effects of stattic (Figure 4C), the inhibitor of STAT3 signaling, which significantly decreased the expression of mature-IL-1β, ASC, AIM2, NLRP3, cleaved-caspase-1 and GSDMD-N in LPS-stimulated microglial cells. However, administration of IL-6 as

a commonly stimulus for activating STAT3 signaling caused the expression of mature-IL-1β, ASC, AIM2, NLRP3, cleaved-caspase-1 and GSDMD-N to rise again compared with the Rg1+LPS group (Figure 4C). Along with mature-IL-1β, ASC, AIM2, NLRP3, cleaved-caspase -1 and GSDMD-N, the rate of apoptosis was decreased after Rg1 pretreatment with LPS stimulation. The anti-apoptosis properties of Rg1 have been previously studied,[44] although there is currently no study on the effect of Rg1 on inflammasome activation–mediated pyroptosis. Pyroptosis is characterized by the rapid loss of the plasma membrane integrity. Therefore, membrane-impermeable dyes like PI will stain the pyroptotic cell. While Annexin V binds to phosphatidyl localized to the inner leaflet of the cell membrane. By Annexin V-FITC and PI staining, we have shown that the percentage of early apoptotic and necrotic or late apoptotic microglial cells induced by LPS was increased by more than two-fold compared with the control group. Very strikingly, Rg1 pretreatment significantly decreased the percentage of early apoptotic and necrotic or late apoptotic cells. As opposed to this, administration of IL-6 (a STAT3 agonist) resulted in a significant increase in the apoptosis ratio. Taken together, it is suggested that Rg1 has a neuroprotective function because it can decrease inflammasome-mediated pyroptosis in microglia challenged by LPS as demonstrated in the present results.

When the AIM2 inflammasomes are activated, AIM2 interacts with ASC via PYD-PYD homotypic interaction and which in turn recruits pro-caspase-1.[45–47] The activation of the AIM2 inflammasome is responsible for processing and secretion of IL-1β and IL-18.[48,49] Inhibition of the activation of the AIM2 inflammasome is associated with improved innate immune responses.[50] To further investigate the activation mechanism of AIM2 in neuroinflammation, STAT3 as a transcription factor and its targeted genes were predicted by hTFtarget database and AIM2 was found. JASPAR website has predicted the sites where STAT3 binds to AIM2. ChIP assay verified that STAT3 might target the predicted site 1 of AIM2 promoter (Figure 4A). Therefore, our findings indicated that STAT3 signaling enhances pyroptosis by further targeting AIM2 inflammasome.

However, unlike AIM2, NLRP3 inflammasome belongs to NLRs family, a different type of inflammasome; it is formed by the sensor pyrin, pyrin interacts with ASC through PYD-PYD homotypic interactions and ASC further recruited caspase1.[51] In this study, we have confirmed that STAT3 could regulate the expression of NLRP3 in activated microglia induced by LPS; however, it remains to be ascertained whether STAT3 has a direct regulatory effect on NLRP3. Studies have shown that PRRs such as Toll-like receptors (TLRs), or NODs and cytokines such as TNF-α trigger the activation of the transcription factor NF-κB which interacts with STAT3, affecting the expression of the inflammasome components NLRP3.[52] Therefore, the mechanism of STAT3 in regulating the expression of NLRP3 needs to be further explored in the future.

Conclusion

The present results have shown that STAT3 plays a pivotal role in regulating the activation cascade of pyroptosis in LPS stimulated microglia. More importantly, we have shown that Rg1 can inhibit STAT3 signaling by interfering with the STAT3 phosphorylation at Tyr705, and through AIM2, it would ultimately lead to inhibition of pyroptosis of microglia. Overall, the present results have provided unequivocal evidence supporting Rg1 as a potential therapeutic agent for amelioration of microglia-mediated neuroinflammatory diseases.

Abbreviations

AD, Alzheimer's disease; AIM2, absent in melanoma 2; ASC, apoptosis-associated speck-like protein containing a CARD; CARD, caspase activation and recruitment domain; CNS, central nervous system; ChIP, chromatin immunoprecipitation; DAMPs, damage-associated molecular patterns; DMEM, Dulbecco's Modified Eagle medium; GSDMD, gasdermin D; GSDMD-N, activated NH (2)-terminal fragment of GSDMD; IL-18, interleukin-18; IL-1β, interleukin-1β; LPS, lipopolysaccharide; MS, multiple sclerosis; NLRs, NOD-like receptors; NLRP3, NOD-, LRR- and pyrin domain-containing 3; PD, Parkinson's disease; PRR, pattern recognition receptor; PPI, protein–protein interaction; PYD, pyrin domain; Rg1, ginsenoside Rg1; STAT, signal transducer and activator of transcription; SDS-PAGE, SDS-polyacrylamide gel electrophoresis; TLRs, Toll-like receptors; tryptophan 705, Tyr705.

Funding

This study was supported by the National Natural Sciences Foundation of China (Grants No. 81960251, 81460210, 81360200), Department project of Science and Technology of Yunnan Province (Grants No. 2018FE001 (-029), 202001AY070001-174) and the Department

project of Education of Yunnan Province (Grant No. 2019J1214).

Disclosure

The authors report no conflicts of interest in this work.

References

1. Chakraborty S, Kaushik DK, Gupta M, Basu A. Inflammasome signaling at the heart of central nervous system pathology. *J Neurosci Res*. 2010;88:1615–1631. doi:10.1002/jnr.22343
2. Nencini P, Sarti C, Innocenti R, Pracucci G, Inzitari D. Acute inflammatory events and ischemic stroke subtypes. *Cerebrovasc Dis*. 2003;15(3):215–221. doi:10.1159/000068831
3. Kierdorf K, Erny D, Goldmann T, et al. Microglia emerge from erythromyeloid precursors via Pu.1- and Irf8-dependent pathways. *Nat Neurosci*. 2013;16(3):273–280. doi:10.1038/nn.3318
4. Ginhoux F, Greter M, Leboeuf M, et al. Fate mapping analysis reveals that adult microglia derive from primitive macrophages. *Science*. 2010;330(6005):841–845. doi:10.1126/science.1194637
5. Alliot F, Godin I, Pessac B. Microglia derive from progenitors, originating from the yolk sac, and which proliferate in the brain. *Brain Res Dev Brain Res*. 1999;117(2):145–152. doi:10.1016/s0165-3806(99)00113-3
6. Saijo K, Glass CK. Microglial cell origin and phenotypes in health and disease. *Nat Rev Immunol*. 2011;11(11):775–787. doi:10.1038/nri3086
7. Latz E, Xiao TS, Stutz A. Activation and regulation of the inflammasomes. *Nat Rev Immunol*. 2013;13(6):397–411. doi:10.1038/nri3452
8. Lamkanfi M, Dixit VM. Mechanisms and functions of inflammasomes. *Cell*. 2014;157(5):1013–1022. doi:10.1016/j.cell.2014.04.007
9. Martinon F, Burns K, Tschopp J. The inflammasome: a molecular platform triggering activation of inflammatory caspases and processing of proIL-beta. *Mol Cell*. 2002;10(4):417–426. doi:10.1016/s1097-2765(02)00599-3
10. Howrylak JA, Nakahira K. Inflammasomes: key mediators of lung immunity. *Annu Rev Physiol*. 2017;79:471–49[illegible] doi:10.1146/annurev-physiol-021115-1052[illegible]
11. Man SM, Kanneganti TD. Regulation of inflammasome activation. *Immunol Rev*. 2015;265(1):6–21. doi:10.1111/imr.12296
12. Liang Y, Jing X, Zeng [illegible] et al. Rifampicin attenuates rotenone-induced inflammation via suppressing nlrp3 inflammasome activation in microglia. *Brain Res*. 2018;1622:43–50. doi:10.1016/j.brainres.2018.06.008
13. Pan Y, Chen XY, Zhang QY, Kong LD. Microglial nlrp3 inflammasome activation mediates il-1β-related inflammation in prefrontal cortex of depressed rats. *Brain Behav Immun*. 2014;41:90–100. doi:10.1016/j.bbi.2014.04.007
14. Hornung V, Latz E. Intracellular DNA recognition. *Nat Rev Immunol*. 2010;10(2):123–130. doi:10.1038/nri2690
15. Wang Y, Mao L, Zhang L, et al. Adoptive regulatory T-cell therapy attenuates Subarachnoid hemorrhage-induced cerebral inflammation by suppressing TLR4/NF-B signaling pathway. *Curr Neurovasc Res*. 2016;13(2):121–126. doi:10.2174/1567202613666160314151536
16. Zhou Y, Wang Y, Wang J, Anne Stetler R, Yang QW. Inflammation in intracerebral hemorrhage: from mechanisms to clinical translation. *Prog Neurobiol*. 2014;115:25–44. doi:10.1016/j.pneurobio.2013.11.003
17. Shi J, Gao W, Shao F. Pyroptosis: gasdermin-mediated programmed necrotic cell death. *Trends Biochem Sci*. 2017;42(4):245–254. doi:10.1016/j.tibs.2016.10.004
18. Bergsbaken T, Fink SL, Cookson BT. Pyroptosis: host cell death and inflammation. *Nat Rev Microbiol*. 2009;7(2):99–109. doi:10.1038/nrmicro2070
19. Fink SL, Cookson BT. Apoptosis, pyroptosis, and necrosis: mechanistic description of dead and dying eukaryotic cells. *Infect Immun*. 2005;73(4):1907–1916. doi:10.1128/IAI.73.4.1907-1916.2005
20. O'Shea JJ, Gadina M, Schreiber RD. Cytokine signaling in 2002: new surprises in the Jak/Stat pathway. *Cell*. 2002;109:S121–S131. doi:10.1016/s0092-8674(02)00701-8
21. Darnell JE. Validating Stat3 in cancer therapy. *Nature Med*. 2005;11(6):595–596. doi:10.1038/nm0605-595
22. Planas AM, Soriano MA, Berruezo M, et al. Induction of Stat3, a signal transducer and transcription factor, in reactive microglia following transient focal cerebral ischaemia. *Eur J Neurosci*. 1996;8(12):2612–2618. doi:10.1111/j.1460-9[illegible]6.tb01556.x
23. Anna MP, Meritxeil B, Caries J, Ba[illegible]on S, Fer[illegible] Stat3 is present in the developing and adult rat cerebellum and participates in the formation of transcription complexes binding DNA at the sis-inducible element. *J Neurochem*. 1997;68(4):[illegible]5–1351. doi:10.1046/j.1471-4159.1997.68041345.x
24. Cattaneo E, Conti L, De-fraja C. Signalling through the JAK-STAT pathway in the developing brain. *Trends Neurosci*. 1999;22(8):365–369. doi:10.1016/0166-2236(98)01378-2
25. Wu CF, Bi[illegible] Yang JY, et al. Differential effects of ginsenosides on NO and TNF-alpha production by LPS-activated N9 microglia. *Int Immunopharmacol*. 2007;7(3):313–320. doi:10.1016/j.intimp.2006.09.021
26. Zong Y, Ai QL, Zhong LM, et al. Ginsenoside Rg1 attenuates lipopolysaccharide-induced inflammatory responses via the phospholipase C signaling pathway in murine BV-2 microglial cells. *Curr Med Chem*. 2012;19(5):770–779. doi:10.2174/092986712792067[illegible]
27. Gao XQ, Du ZR, Yuan LJ, et al. Ginsenoside Rg1 exerts anti-inflammatory effects via G protein-coupled estrogen receptor in lipopolysaccharide-induced microglia activation. *Front Neurosci*. 2019;13:1168. doi:10.3389/fnins.2019.01168
28. Lu D, Bai XC, Gui L, et al. Hydrogen peroxide in the Burkitt's lymphoma cell line Raji provides protection against arsenic trioxide-induced apoptosis via the phosphoinositide-3 kinase signalling pathway. *Br J Haematol*. 2004;125(4):512–520. doi:10.1111/j.1365-2141.2004.04940.x
29. Sandelin A, Alkema W, Engström P, Wasserman WW, Lenhard B. JASPAR: an open-access database for eukaryotic transcription factor binding profiles. *Nucleic Acids Res*. 2004;32(Database issue):D91–D94. doi:10.1093/nar/gkh012
30. Hong X, Song R, Song H, et al. PTEN antagonises Tcl1/hnrnpk-mediated G6PD pre-mRNA splicing which contributes to hepatocarcinogenesis. *Gut*. 2014;63(10):1635–1647. doi:10.1136/gutjnl-2013-305302
31. Gao J, Wan F, Tian M, et al. Effects of ginsenoside-Rg1 on the proliferation and glial-like directed differentiation of embryonic rat cortical neural stem cells in vitro. *Mol Med Rep*. 2017;16(6):8875–8881. doi:10.3892/mmr.2017.7737
32. Luo M, Yan D, Sun Q, et al. Ginsenoside Rg1 attenuates cardiomyocyte apoptosis and inflammation via the TLR4/NF-kB/NLRP3 pathway. *J Cell Biochem*. 2020;121(4):2994–3004. doi:10.1002/jcb.29556
33. Li C, Wang X, Kuang M, et al. UFL1 modulates NLRP3 inflammasome activation and protects against pyroptosis in LPS-stimulated bovine mammary epithelial cells. *Mol Immunol*. 2019;112:1–9. doi:10.1016/j.molimm.2019.04.023
34. Ye JX, Wang M, Wang RY, et al. Hydroxysafflor yellow A inhibits hypoxia/reoxygenation-induced cardiomyocyte injury via regulating the AMPK/NLRP3 inflammasome pathway. *Int Immunopharmacol*. 2020;82:106316. doi:10.1016/j.intimp.2020.106316

35. Reinke S, Linge M, Diebner HH, et al. Non-canonical Caspase-1 signaling drives RIP2-Dependent and TNF-α-mediated inflammation in vivo. *Cell Rep*. 2020;30(8):2501–2511. doi:10.1016/j.celrep.2020.01.090
36. Kreutzberg GW. Microglia: a sensor for pathological events in the CNS. *Trends Neurosci*. 1996;19(8):312–318. doi:10.1016/0166-2236(96)10049-7
37. O'Shea JJ, Holland SM, Staudt LM. Jaks and stats in immunity, immunodeficiency, and cancer. *N Engl J Med*. 2013;368(2):161–170. doi:10.1056/NEJMra1202117
38. Yu L, Chen C, Wang LF, et al. Neuroprotective effect of kaempferol glycosides against brain injury and neuroinflammation by inhibiting the activation of nf-kappab and stat3 in transient focal stroke. *PLoS One*. 2013;8(2):e55839. doi:10.1371/journal.pone.0055839
39. Ziv Y, Ron N, Butovsky O, et al. Immune cells contribute to the maintenance of neurogenesis and spatial learning abilities in adulthood. *Nat Neurosci*. 2006;9(2):268–275. doi:10.1038/nn1629
40. Urrutia PJ, Mena NP, Núñez MT. The interplay between iron accumulation, mitochondrial dysfunction, and inflammation during the execution step of neurodegenerative disorders. *Front Pharmacol*. 2014;5:38. doi:10.3389/fphar.2014.00038
41. Zhang WH, Wang X, Narayanan M, et al. Fundamental role of the Rip2/caspase-1 pathway in hypoxia and ischemia-induced neuronal cell death. *Proc Natl Acad Sci U S A*. 2003;100(26):16012–16017. doi:10.1073/pnas.2534856100
42. Shi J, Zhao Y, Wang K, et al. Cleavage of GSDMD by inflammatory caspases determines pyroptotic cell death. *Nature*. 2015;526(7575):660–665. doi:10.1038/nature15514
43. He WT, Wan H, Hu L, et al. Gasdermin D is an executor of pyroptosis and required for interleukin-1 secretion. *Cell Res*. 2015;25(12):1285–1298. doi:10.1038/cr.2015.139
44. Lu D, Zhu LH, Shu XM, et al. Ginsenoside Rg1 relieves tert-Butyl hydroperoxide-induced cell impairment in mouse microglial BV2 Cells. *J Asian Nat Prod Res*. 2015;17(9):930–945. doi:10.1080/10286020.2015.1031117
45. Jin T, Perry A, Smith P, Jiang J, Xiao TS. Structure of the absent in melanoma 2 (AIM2) pyrin domain provides insights into the mechanisms of AIM2 autoinhibition and inflammasome assembly. *J Biol Chem*. 2013;288(19):13225–13235. doi:10.1074/jbc.M113.468033
46. Jin T, Perry A, Jiang J, et al. Structures of the HIN domain: DNA complexes reveal ligand binding and activation mechanisms of the AIM2 inflammasome and IFI16 receptor. *Immunity*. 2012;36(4):561–571. doi:10.1016/j.immuni.2012.02.014
47. Schroder K, Tschopp J. The inflammasomes. *Cell*. 2010;140(6):821–832. doi:10.1016/j.cell.2010.01.040
48. Rathinam VA, Jiang Z, Waggoner SN, et al. The AIM2 inflammasome is essential for host defense against cytosolic bacteria and DNA viruses. *Nat Immunol*. 2010;11(5):395–402. doi:10.1038/ni.1864
49. Hu S, Peng L, Kwak YT, et al. The DNA sensor AIM2 maintains intestinal homeostasis via regulation of epithelial antimicrobial host defense. *Cell Rep*. 2015;13(9):1922–1936. doi:10.1016/j.celrep.2015.10.040
50. Zhang H, Luo J, Alcorn JF, et al. AIM2 inflammasome is critical for influenza-induced lung injury and mortality. *J Immunol*. 2017;198:4383–4393. doi:10.4049/jimmunol.1600714
51. Heilig R, Dick MS, Sborgi L, et al. The Function and mechanism of the pyrin inflammasome. *Eur J Immunol*. 2018;48(2):230–238. doi:10.1002/eji.201746947
52. He Y, Hara H, Li XM, Liu Z, Wang P, Wang BE. HMGB1 promotes the synthesis of pro-IL-1β and pro-IL-18 by activation of p38 MAPK and NF-κB through receptors for advanced glycation end-products in macrophages. *Asian Pac J Cancer Prev*. 2012;13(4):1365–1370. doi:10.7314/apjcp.2012.13.4.1365